Dalton Transactions

PAPER

View Article Online
View Journal | View Issue

Cite this: *Dalton Trans.*, 2014, **43**, 8690

Dimeric 1,3-propanediaminetetraacetato lanthanides as the precursors of catalysts for the oxidative coupling of methane†

Mao-Long Chen, Yu-Hui Hou, Wen-Sheng Xia, Wei-Zheng Weng, Ze-Xing Cao,* Zhao-Hui Zhou* and Hui-Lin Wan

Received 13th January 2014,
Accepted 25th February 2014

DOI: 10.1039/c4dt00104d

www.rsc.org/dalton

From neutral solutions, dimeric 1,3-propanediaminetetraacetato lanthanides $(NH_4)_2[Ln_2(1,3\text{-pdta})_2(H_2O)_4]\cdot 8H_2O$ [Ln = La, **1**; Ce, **2**] and $K_2[Ln_2(1,3\text{-pdta})_2(H_2O)_4]\cdot 11H_2O$ [Ln = La, **3**; Ce, **4**] (1,3-H_4pdta = 1,3-propanediaminetetraacetic acid, $C_{11}H_{18}N_2O_8$) were isolated in high yields. The reaction of excess strontium nitrate with **1** resulted in the formation of a two dimensional coordination polymer $[La_2(1,3\text{-pdta})_2(H_2O)_4]_n\cdot[Sr_2(H_2O)_6]_n\cdot[La_2(1,3\text{-pdta})_2(H_2O)_2]_n\cdot 18nH_2O$ (**5**) at 70 °C. Complexes **1–4** show a similar central molecular structure. The lanthanide ions are coordinated by two nitrogen atoms, four carboxy oxygen atoms from one 1,3-pdta ligand, two from the neighboring 1,3-pdta ligand forming a four-membered ring and two water molecules. Complex **5** has two kinds of dimeric lanthanum unit and extends into a 2D coordination polymer through strontium ions and bridged oxygen atoms, and forms a fourteen membered ring linked by oxygen atoms from carboxy groups of pdta. Complexes **1–4** are soluble in water. The $^{13}C\{^1H\}$ NMR experiments for complex **1** were tested in solution. Thermal products from **1** and **5** show good catalytic activities towards the oxidative coupling reaction of methane (OCM). The conversion of methane and selectivity to C_2 reached 29.7% and 51.7% at 750 °C for the product of **5**. From TGA, XRD and SEM analyses, the thermal products from **1** and **5** are rod- and poly-shaped, which are assigned as lanthanum oxocarbonate and a mixture of La_2O_3, $SrCO_3$ and $La_2O_2CO_3$ for **1** and **5**, respectively. The precursor method is favorable for the formation of regular shaped mixed oxides.

Introduction

Recently, lanthanide coordination complexes have attracted increasing attention because of their interesting properties such as magnetism,[1] optical properties,[2] and use as complexing agents in the separation of lanthanide cations,[3] contrast agents in magnetic resonance imaging,[4] and precursors for the syntheses of nanoparticles.[5] Lanthanide oxides-based and/or doped nanoparticles represent an interesting investigation field, which can be used as catalysts and supports for noble metal catalysts.[6] For example, lanthanum oxide has applications in solid oxide fuel cells and the oxidative coupling of methane (OCM).[7] Metal oxides can be synthesized in several ways such as: sol–gel,[8] carbonate,[9] templates,[10] homogeneous precipitation,[11] thermal treatments of the precursors of coordination complexes,[12] *etc.* Among them, the thermal treatment of the precursor method is attractive, since it consists of a moderate calcinating temperature with explicit composition, yielding high purity oxides. In general, 1,3-propanediaminetetraacetic acid {1,3-H_4pdta = $CH_2[CH_2N(CH_2CO_2H)_2]_2$} which is a edta-like ligand {edta = $[CH_2N(CH_2CO_2H)_2]_2$} is a tetrabasic acid with eight potential O-donor and two N-donor atoms. Compared with transition metals, lanthanide ions have a high coordination number (CN) and coordination flexibility. Combination of 1,3-pdta and the high CN of lanthanides might be expected to isolate different sorts of lanthanide complexes, which can be used as precursors in thermal treatment processes. In a previous paper, we reported an interesting metal–organic framework (MOF) structure constructed by lanthanum and 1,3-pdta, which demonstrated a potential use for low-pressure desalination.[13] Herein, four dimeric hydrated 1,3-propanediaminetetraacetato lanthanides $(NH_4)_2[Ln_2(1,3\text{-pdta})_2(H_2O)_4]\cdot 8H_2O$ [Ln = La, **1**; Ce, **2**] and $K_2[Ln_2(1,3\text{-pdta})_2(H_2O)_4]\cdot 11H_2O$ [Ln = La, **3**; Ce, **4**] were isolated in high yields.

State Key Laboratory of Physical Chemistry of Solid Surfaces, College of Chemistry and Chemical Engineering, Xiamen University, Xiamen, 361005, China.
E-mail: zxcao@xmu.edu.cn, zhzhou@xmu.edu.cn; Fax: +86 592 2183047; Tel: +86 592 2184531

†Electronic supplementary information (ESI) available: Ortep figures of **2–4** (Fig. S1–S3), 3D supramolecular network of **5** (Fig. S4); solution ^1H NMR spectra of H_4pdta and **1** (Fig. S5 and S6); IR vibrational spectra (Fig. S7–S11); TG-DTG curves of **1** (Fig. S12) and the catalytic activities data (Table S1). CCDC 974203–974207. For ESI and crystallographic data in CIF or other electronic format see DOI: 10.1039/c4dt00104d

With excess strontium nitrate, a two dimensional coordination polymer $[La_2(1,3\text{-pdta})_2(H_2O)_4]_n{\cdot}[Sr_2(H_2O)_6]_n{\cdot}[La_2(1,3\text{-pdta})_2(H_2O)_2]_n{\cdot}18nH_2O$ (**5**) was isolated from **1**. The thermal analysis of **1** and **5** was investigated, and their thermal decomposition products show good catalytic activities towards the oxidative coupling of methane.

Experimental

Materials and instrumentation

All chemicals were of analytical or reagent-grade purity and used as received. The pH value was measured by the potentiometric method with a PHB-8 digital pH meter. Elemental analyses (C, H, N) were performed by an EA1110 elemental analyzer. Infrared spectra were recorded as KBr disks and as mulls in Nujol with a Nicolet 330 FT-IR spectrophotometer. SEM images were recorded on HITACHI S-4800 electron microscope. Thermogravimetric analysis were recorded on a SDT-Q600 thermal analyzer, under an air flow of 100 mL·min^{-1} at a heating rate of 10 °C·min^{-1}. Solution $^{13}C\{^1H\}$ NMR spectra were recorded in D_2O on a Bruker AV 400 M NMR spectrometer using DSS (sodium 2,2-dimethyl-2-silapentane-5-sulfonate) as the internal reference. Powder X-ray diffraction (XRD) data were collected using monochromated Cu Kα radiation on a Phillips X'Pert diffractometer.

Synthesis

Preparation of dimeric $(NH_4)_2[La_2(1,3\text{-pdta})_2(H_2O)_4]{\cdot}8H_2O$ (1) and $(NH_4)_2[Ce_2(1,3\text{-pdta})_2(H_2O)_4]{\cdot}8H_2O$ (2). $LaCl_3{\cdot}7H_2O$ (0.74 g, 2.0 mmol) and H_4pdta (0.62 g, 2.0 mmol) were dissolved in water (15 mL) and stirred for 1.5 h. The pH value of the reaction mixture was adjusted to 6.5 with 5.0 M ammonium hydroxide, and heated at 70 °C for 12 h. The mixture was left to stand at room temperature. A colorless crystalline material was separated from the evaporated solution, and was washed with cold water and ethanol, then dried under a vacuum. The yield was 61% (0.75 g). Anal. Found (calcd for $C_{22}H_{60}La_2N_6O_{28}$): C, 23.4 (23.2); H, 5.1 (5.3); N, 7.2 (7.4). IR (KBr disk, /cm^{-1}): 3443_{vs}, 3243_{vs}, 2977_s, $\nu_{as}(CO_2)$, 1585_{vs}; $\nu_s(CO_2)$, 1408_{vs}, 1333_s, 1310_s, 1262_m; 1157_m, 1113_m, 1067_w, 1013_w, 986_w, 964_w, 931_m, 862_w, 772_m, 742_m, 703_m, 614_m, 568_m, 509_w, 439_w. Solution ^1H NMR (500 MHz, D_2O): δ (ppm) 3.311 (8H, s), 2.689 (4H, t, J = 5.0 Hz), 1.688 (2H, m); ^{13}C NMR (500 MHz, D_2O): δ (ppm) 182.7 (–CO_2), 65.1 (–CH_2CO_2), 62.2 (–NCH_2–), 24.9 (–CH_2–). Preparation of cerium complex **2** was similar to that of **1**. The yield was 65% (0.74 g). Anal. Found (calcd for $C_{22}H_{60}Ce_2N_6O_{28}$): C, 23.5 (23.2); H, 5.0 (5.3); N, 7.3 (7.4). IR (KBr disk, /cm^{-1}): 3439_s, 3221_s, $\nu_{as}(CO_2)$, 1589_{vs}; $\nu_s(CO_2)$, 1409_s, 1381_s, 1336_m, 1309_m; 1264_w, 1243_w, 1158_w, 1111_w, 1067_w, 1015_w, 985_w, 964_w, 928_m, 863_w, 776_w, 742_m, 706_w, 614_m, 564_w.

Preparation of $K_2[La_2(1,3\text{-pdta})_2(H_2O)_4]{\cdot}11H_2O$ (3) and $K_2[Ce_2(1,3\text{-pdta})_2(H_2O)_4]{\cdot}11H_2O$ (4). $LaCl_3{\cdot}7H_2O$ (0.74 g, 2.0 mmol) and H_4pdta (0.62 g, 2.0 mmol) were dissolved in water (15 mL) and stirred for 1.5 h. The pH value of the reaction mixture was adjusted to 6.5 with 5.0 M potassium hydroxide and heated at 70 °C for 12 h. The mixture was left to stand in the air at room temperature. A colorless crystalline material was separated from the evaporated solution, and was washed with cold water and ethanol, then dried under a vacuum. The yield was 76% (0.94 g). Anal. Found (calcd for $C_{22}H_{58}K_2La_2N_4O_{31}$): C, 21.4 (21.5); H, 4.7 (4.7); N, 4.5 (4.6). IR (KBr disk, /cm^{-1}): 3432_s, $\nu_{as}(CO_2)$, 1616_{vs}; $\nu_s(CO_2)$, 1409_s, 1391_s, 1336_s, 1301_m; 1262_m, 1157_w, 1124_w, 1075_w, 1024_w, 996_w, 931_m, 918_m, 876_m, 739_m, 607_m, 561_m, 424_w. Preparation of cerium complex **4** was similar to that of **3**. The yield was 69% (0.85 g). Anal. Found (calcd for $C_{22}H_{58}K_2Ce_2N_4O_{31}$): C, 21.7 (21.4); H, 4.6 (4.7); N, 4.6 (4.5). IR (KBr disk, /cm^{-1}): 3388_s, $\nu_{as}(CO_2)$, 1589_{vs}; $\nu_s(CO_2)$, 1416_s, 1341_s, 1310_s, 1264_m; 1238_m, 1094_m, 1027_w, 991_w, 924_m, 879_w, 814_m, 723_s, 655_s, 532_m, 505_m, 447_w.

Preparation of $[La_2(1,3\text{-pdta})_2(H_2O)_4]_n{\cdot}[Sr_2(H_2O)_6]_n{\cdot}[La_2(1,3\text{-pdta})_2(H_2O)_2]_n{\cdot}18nH_2O$ (5). $(NH_4)_2[La_2(1,3\text{-pdta})_2(H_2O)_4]{\cdot}8H_2O$ (**1**) (2.26 g, 2.0 mmol) was dissolved in water (20 mL) and stirred for 1.5 h. $Sr(NO_3)_2$ (0.85 g, 4.0 mmol) was added to the solution and stirred at 70 °C for several minutes. The mixture was left standing at 70 °C under sealed conditions. A colorless crystalline material was separated from the evaporated solution, and was washed with cold water and ethanol, then dried under a vacuum. The yield was 68% (1.69 g). Anal. Found (calcd for $C_{44}H_{116}La_4N_8O_{62}Sr_2$): C, 21.7 (21.4); H, 4.6 (4.7); N, 4.8 (4.5). IR (KBr disk, /cm^{-1}): 3426_s, 2955_m, 2853_m; $\nu_{as}(CO_2)$, 1581_{vs}; $\nu_s(CO_2)$, 1449_m, 1409_s; 1329_m, 1307_w, 1260_w, 1161_w, 1113_w, 1069_w, 1018_w, 989_w, 939_w, 868_w, 793_w, 718_m, 615_m, 567_w.

Catalytic reaction

The catalytic performances of the catalysts were investigated using a CH_4/O_2 = 2.8/1 mixture (molar ratio) as a reaction feed. The OCM reaction for the investigated samples was carried out in a fixed-bed quartz tubular reactor (internal diameter 5 mm) at atmospheric pressure and a total flow rate of 50 mL·min^{-1}. The reactor was packed with 0.2 g samples (40–60 mesh sizes) between quartz wool plugs. The reactor was heated with a furnace connected to a temperature controller (Yudian AI-708PFKSL2). The performances of the catalysts were evaluated over the temperature range of 550–800 °C with a gas hourly space velocity (GHSV) of 15 000 mL·g^{-1}·h^{-1}.

X-Ray crystallography

Suitable single crystals of **1–5** were selected and quickly mounted onto thin glass fibers to prevent the loss of water molecules. The X-ray intensity data for complexes **2–5** were measured at 173 K (**1** was measured at 153 K) on a Oxford CCD diffractometer with Mo Kα radiation (λ = 0.71073 Å). Empirical adsorption was applied to all data using SADABS and CrysAlis (multi-scan) programs. The initial model was obtained through direct methods and the completion of the rest of the structure was achieved by difference Fourier strategies. The structures were refined by least squares on F^2, with anisotropic displacement parameters for non-H atoms. Most of the hydrogen atoms unambiguously defined by the stereochemistry were

Table 1 Crystal data and structural refinements for **1–5**[a]

Compound reference	**1**	**2**	**3**	**4**	**5**
Chemical formula	$C_{22}H_{60}La_2N_6O_{28}$	$C_{22}H_{60}Ce_2N_6O_{28}$	$C_{22}H_{58}La_2N_4O_{31}K_2$	$C_{22}H_{58}Ce_2N_4O_{31}K_2$	$C_{44}H_{116}La_4N_8O_{62}Sr_2$
Formula mass	1134.58	1137.00	1230.74	1233.16	2480.33
Crystal system	Triclinic				
a/Å	9.1820(2)	9.1815(4)	9.0362(3)	9.0204(5)	10.8949(3)
b/Å	10.7781(3)	10.7611(4)	10.8215(4)	10.7890(6)	14.4341(4)
c/Å	11.3519(3)	11.3292(4)	11.7411(3)	11.7467(5)	15.4414(5)
α/°	101.512(2)	101.806(3)	80.775(3)	80.869(4)	72.312(3)
β/°	105.284(2)	105.137(3)	80.888(2)	80.717(4)	71.264(3)
γ/°	100.003(2)	99.966(3)	76.343(3)	76.388(5)	76.982(2)
Unit cell volume/Å^3	1031.01(5)	1026.83(7)	1092.49(6)	1087.8(1)	2168.8(1)
Temperature/K	153(2)	173(2)			
Space group	$P\bar{1}$				
No. of formula units per unit cell, Z	1				
Radiation type	MoKα				
Absorption coefficient, μ/mm^{-1}	2.145	2.290	2.222	2.360	3.262
No. of reflections measured	10 792	9075	9917	12 971	29 946
No. of independent reflections	5223	4252	4769	4979	9380
R_{int}	0.0397	0.0394	0.0280	0.0345	0.0586
Final R_1 values ($I > 2\sigma(I)$)	0.0294	0.0245	0.0262	0.0225	0.0390
Final w$R(F^2)$ values ($I > 2\sigma(I)$)	0.0698	0.0548	0.0639	0.0448	0.0710
Final R_1 values (all data)	0.0353	0.0285	0.0291	0.0281	0.0517
Final w$R(F^2)$ values (all data)	0.0723	0.0560	0.0653	0.0455	0.0753
Goodness of fit on F^2	0.938	1.025	1.020	1.002	1.051

[a] $R_1 = \sum||(F_o| - |F_c||/(\sum|F_o|$, $wR_2 = \{\sum[w(F_o^2 - F_c^2)^2]/\sum[w(F_o^2)^2]\}^{1/2}$.

placed at their calculated positions and allowed to ride onto their host carbons both in coordinates as well as in thermal parameters (C–H, 0.97 Å). Those attached to oxygen and needed for the H-bonding description were located in a late Fourier map and refined with similarity restrains [O–H, 0.85(1) Å; H···H, 1.39(1) Å]. All calculations to solve and refine the structures and to obtain derived results were carried out with the computer programs SHELXS 97, and SHELXL 97 programs. Full use of the CCDC package was also made for searching in the CSD Database.[14] CCDC deposition numbers are 974203–974207.† Crystal data and structure refinements for **1–5** are summarized in Table 1.

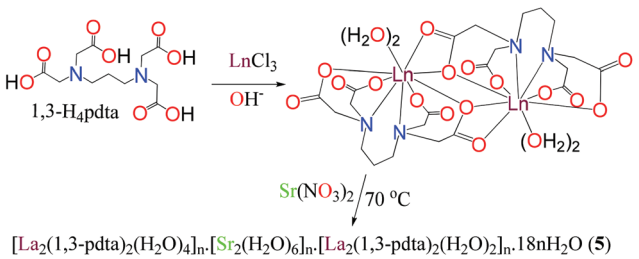

Scheme 1 Preparation and conversion of 1,3-propanediaminetetraacetato lanthanides in different neutral solutions (Ln = La or Ce).

Results and discussion

The syntheses of complexes **1–5** were carried out in neutral aqueous solutions with different cations. In **1–4**, it was found that potassium salts combined with much more crystallized water molecules. When excess $Sr(NO_3)_2$ was added to the solution of **1**, a two-dimensional coordination polymer $[La_2(1,3\text{-pdta})_2(H_2O)_4]_n{\cdot}[Sr_2(H_2O)_6]_n{\cdot}[La_2(1,3\text{-pdta})_2(H_2O)_2]_n{\cdot}18nH_2O$ (**5**) was isolated in warm solution (70 °C), as shown in Scheme 1.

Crystal structure descriptions

Fig. 1 shows the anion structure of $(NH_4)_2[La_2(1,3\text{-pdta})_2(H_2O)_4]{\cdot}8H_2O$ (**1**). Anion structures of **2–4** are similar to that of **1**, which are shown in Fig. S1–S3.†

X-Ray structural analysis revealed that dimeric complexes **1–4** have similar anionic structures. Each Ln(III) cation exists in a decadentate coordination environment, which is different from those of usual nonadentate coordinations in lanthanide

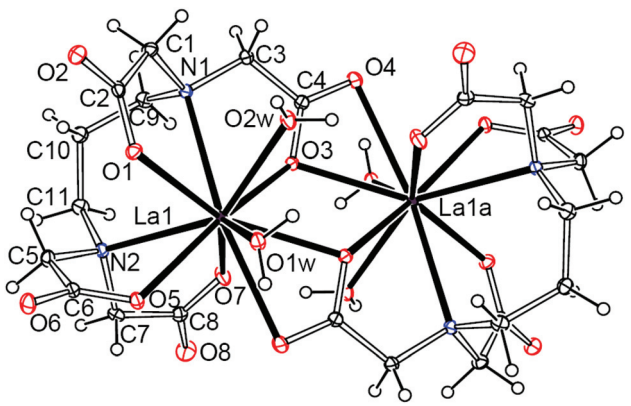

Fig. 1 Anion structure of dimeric complex $(NH_4)_2[La_2(1,3\text{-pdta})_2(H_2O)_4]{\cdot}8H_2O$ (**1**).

ethylenediaminetetraacetates,[7] and is also different from most lanthanide propanediaminetetraacetates. Here the flexible pdta ligand plays an important role in the formation of the

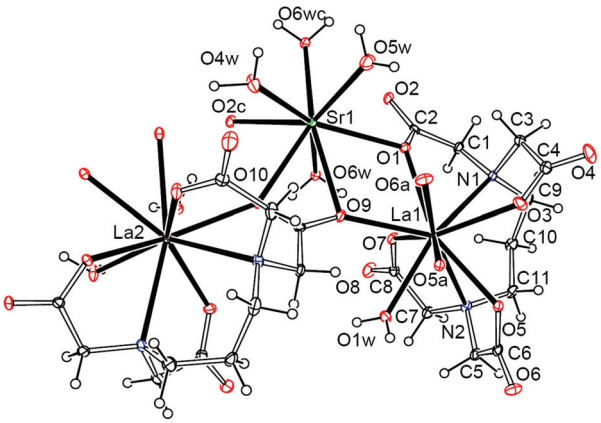

Fig. 2 Molecular structure of $[La_2(1,3\text{-pdta})_2(H_2O)_4]_n{\cdot}[Sr_2(H_2O)_6]_n{\cdot}[La_2(1,3\text{-pdta})_2(H_2O)_2]_n{\cdot}18nH_2O$ (**5**) in an asymmetric unit in 30% thermal ellipsoids.

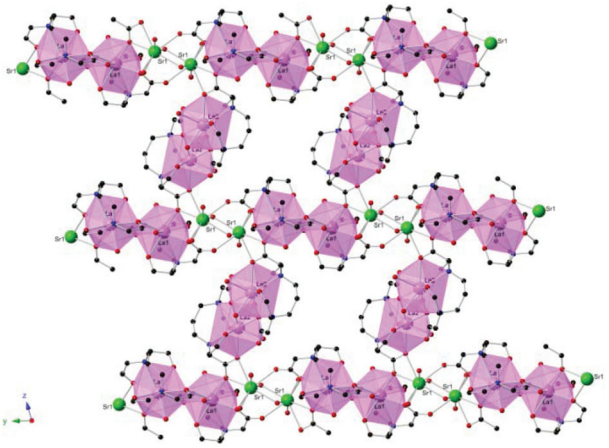

Fig. 3 The infinite 2D structure of $[La_2(1,3\text{-pdta})_2(H_2O)_4]_n{\cdot}[Sr_2(H_2O)_6]_n{\cdot}[La_2(1,3\text{-pdta})_2(H_2O)_2]_n{\cdot}18nH_2O$ (**5**).

decadentate coordination environment. Usually, lanthanum or cerium ethylenediaminetetraacetates with rigid ethylene chains are often observed with a nonadentate coordination number. Moreover, the type of lanthanide also plays a key role. Early lanthanides like La, Ce, Pr and Nd form decadentate coordination numbers more easily than those of heavy lanthanides with short ion radii due to lanthanide contraction. Pdta acts as an octadentate ligand. It uses two nitrogen atoms and four oxygen atoms of acetates to chelate one lanthanide ion. While one of the carboxy group forms a four-membered ring with the other lanthanum ion, forming a dimeric structure as shown in Fig. 1.

Molecular structure of $[La_2(1,3\text{-pdta})_2(H_2O)_4]_n{\cdot}[Sr_2(H_2O)_6]_n{\cdot}[La_2(1,3\text{-pdta})_2(H_2O)_2]_n{\cdot}18nH_2O$ (**5**) is shown in Fig. 2. In **5**, there are two kinds of lanthanum ions existing in different environments. The pdta ligand acts as a ten-dentate and eleven-dentate ligand for two kinds of lanthanum ions, respectively, which is unusual in pdta complexes. Two La1 ions, two 1,3-pdta ligands and two water molecules form a dimeric unit $La_2(1,3\text{-pdta})_2(H_2O)_2$ (unit 1), and two La2 ions, two 1,3-pdta ligands and four water molecules form another dimeric unit $La_2(1,3\text{-pdta})_2(H_2O)_4$ (unit 2), which is similar to that of the former dimeric complexes. As shown in Fig. 3, we can clearly see this two kinds of dimeric lanthanum units. From Fig. 2, we can see half of unit 1 still uses its two oxygen atoms of one carboxy group to coordinate with two strontium ions, and half of unit 2 uses its one carboxy group to chelate with the strontium and bridged with La1 of unit 1. Two strontium ions were bridged by coordinated water molecules (O6w). These make **5** form a two dimensional coordination polymer.

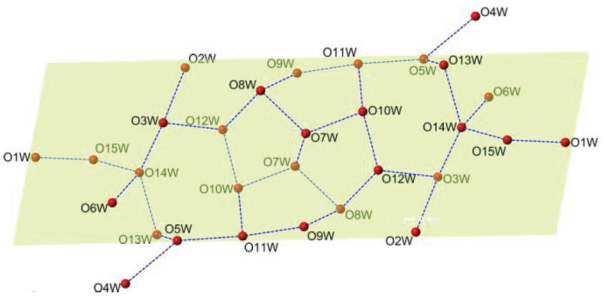

Fig. 4 The coordinated and crystallized water molecules in $[La_2(1,3\text{-pdta})_2(H_2O)_4]_n{\cdot}[Sr_2(H_2O)_6]_n{\cdot}[La_2(1,3\text{-pdta})_2(H_2O)_2]_n{\cdot}18nH_2O$ (**5**), forming a thirty membered water cluster.

As shown in Fig. 4, the crystallized and coordinated water molecules form a thirty membered water molecule cluster. The water molecules were cleaved equally by one plane. These hydrogen bonds and the other hydrogen bonds between the water molecules and carboxy oxygen atoms form a two dimensional network that extends to a three dimensional supramolecular network, as shown in Fig. S4.†

Selected bond lengths for complexes **1–5** are listed in Table 2. The average La–O bond length in dimeric **1** is 2.531(2) Å, and the bond lengths of the bridged four membered ring

Table 2 Selected bond lengths (Å) for **1–4** and **5**

Compound entry	Ln–$O_{\beta\text{-carboxy}}$(av)	Ln–$O_{\beta\text{-bridged}}$	Ln–N(av)	Ln–Ow (av)
1	2.531(2)	2.591(2), 2.773(2)	2.840(2)	2.574(2)
2	2.506(2)	2.566(2), 2.760(2)	2.827(2)	2.552(2)
3	2.531(2)	2.589(2), 2.774(2)	2.832(2)	2.584(2)
4	2.509(2)	2.566(2), 2.763(2)	2.817(2)	2.570(2)
5-unit 1	2.542(3)	2.572(3), 2.672(3), 2.779(3)	2.864(4)	2.504(3)
5-unit 2	2.555(3)	2.644(3), 2.696(3)	2.861(4)	2.557(3)
		Sr–$O_{\beta\text{-bridged}}$(av)		Sr–Ow(av)
5-Sr	—	2.663(3)	—	2.584(3)

are 2.591(2) and 2.773(2) Å. The average La–N and La–Ow bond lengths are 2.840(2) and 2.574(2) Å, respectively. The corresponding bond lengths in lanthanum complex **3** are 2.531(2), 2.589(2), 2.774(2), 2.832(2) and 2.584(2) Å. The two lanthanum complexes are very similar. The La–N bond lengths in **3** are shorter, while La–Ow are longer than those of **1**. In isomorphous cerium dimeric complexes **2** and **4**, the corresponding bond lengths are 2.506(2), 2.566 (2), 2.760(2), 2.827(2) and 2.552(2) Å for **2** and 2.509(2), 2.566 (2), 2.763(2), 2.817(2) and 2.570(2) Å for **4**, respectively. The bond lengths in the two cerium complexes clearly demonstrate the lanthanide contraction effect. In complex **5**, with two kinds of lanthanum ions, the coordinate bonds must be divided into two kinds in order to show the features more clearly. La1 and La2 are both deca-coordinated. La1 ion has an average La1–O bond length [2.542(3) Å] for four oxygen atoms from one pdta ligand and 2.553(3) Å for La2 ion. When involving the bridged carboxy, there exists longer La1–O bond lengths [2.572(3), 2.672(3) and 2.779(3) Å] and longer La1–N bond lengths [2.864(4) Å]. For unit 2, the bond distance with only one water molecule is 2.504(3) Å. This is the shortest La–Ow bond in the five complexes.

NMR analyses

The solution ^{13}C NMR spectra of **1** and H_4pdta are shown in Fig. 5. The pH values of the solutions were around 6.4. The solution ^{1}H NMR spectra are listed in Fig. S5 and S6.† When we compare the ^{13}C NMR spectrum of **1** with that of H_4pdta, obvious downfield shifts show the coordination of pdta ligands. Only one set of ^{13}C NMR chemical shift data was observed for **1**. All carboxy groups give only one ^{13}C NMR signal at 182.7 ppm ($\Delta\delta$ = 10.8 ppm) and one CH_2CO_2 signal at 65.1 ppm ($\Delta\delta$ = 6.3 ppm). Large downfield shifts were observed. From the molecular structure in the solid state, there are two kinds of carboxy groups, but only one peak was observed for the carboxy groups in solution. This should result from the dissociation of the less strongly bridged carboxy group and the formation of a monomeric species in the solution, as shown in Scheme 2. There is also only one set of signals for –CH_2N– (62.2 ppm, $\Delta\delta$ = 6.4 ppm) and –CH_2– (24.9 ppm, $\Delta\delta$ = 2.7 ppm). All in all, the bridged carboxy of pdta in the dimeric lanthanum complexes must dissociate to give a monomeric unit.

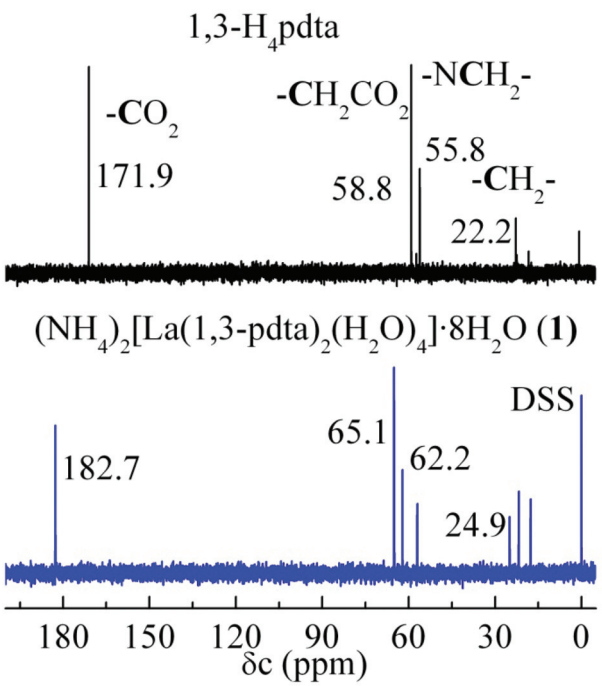

Fig. 5 Solution ^{13}C NMR spectra of 1,3-H_4pdta and $(NH_4)_2[La_2(1,3\text{-pdta})_2(H_2O)_4]\cdot 8H_2O$ (**1**).

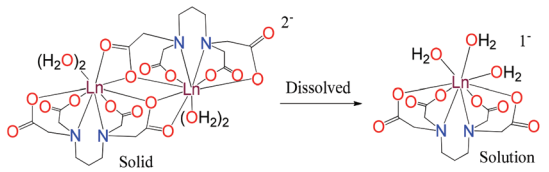

Scheme 2 Conversion of dimeric 1,3-propanediaminetetraacetato lanthanides into monomers when dimeric complexes were dissolved in water.

The dissociation of the dimeric complexes to a monomeric unit in solution should mainly come from the less strongly bridged carboxy groups [La–$O_{\beta\text{-bridged}}$(av) 2.682(2), and 2.682(2) Å for dimeric lanthanum complexes **1** and **3**; 2.630(2) and 2.665(2) Å for **2** and **4** of dimeric cerium complexes], which are easily attacked and substituted by water molecules, compared with the bond distances of normal coordinated β-carboxy groups [La–O(av) 2.531(2) and 2.531(2) Å for dimeric lanthanum complexes **1** and **3**; 2.506(2) and 2.509(2) Å for **2** and **4** of dimeric cerium complexes].

In the ^{1}H NMR spectrum of H_4pdta (Fig. S5†), the eight acetate protons are equivalent and result in one signal at 4.061 ppm. The four –CH_2N– protons are equivalent and result in a tri-signal centred at 3.433 ppm and the two protons of –CH_2– give a penta-signal centred at 2.249 ppm. When we compare the ^{1}H NMR spectra of H_4pdta and lanthanum complex **1**, we find that they give only one set of signals assigned to the different –CH_2– groups, which is consistent with the ^{13}C NMR spectra. 3.311 (8H, s), 2.689 (4H, t, J = 5.0 Hz), 1.688 (2H, m); through the ^{1}H NMR spectrum of **1** (Fig. S6†), a singlet at 3.311 ppm (8H, s, $\Delta\delta$ = −0.750 ppm) for acetate protons and a tri-signal centred at 2.689 ppm (4H, t, J = 7.5 Hz, $\Delta\delta$ = −0.744 ppm) for the –CH_2N– protons and multiple peaks centred at 1.688 (2H, m, $\Delta\delta$ = –0.561 ppm). There are big shifts of the $\Delta\delta$ values for **1**. This is also an indication of the strong coordination of the 1,3-pdta ligand in **1**. Moreover, these also indicate the dissociation of bridged carboxy groups in **1**. This is because only one set of signals was observed for the –CO_2–, –CH_2CO_2, –CH_2N– and –CH_2-groups. Theses results are consistent with the ^{13}C NMR measurements.

Vibrational spectra

The IR vibrational spectra of **1–5** are listed in Fig. S7–S11.† In the region between 1616 and 1581 cm^{-1} and between 1449 and 1330 cm^{-1}, complexes **1–5** give two typical bands that correspond to the bound carboxy groups $\nu_{as}(COO^-)$ and $\nu_s(COO^-)$, respectively. The value of $[\nu(COO^-)_{asp} - \nu(COO^-)_s]$ is about 173 cm^{-1} for **1**, suggesting that the coordination of the carboxy groups is most probably of the bridging type.[15] This is also observed for complexes **2–4**. In **5**, the value of $[\nu(COO^-)_{as} - \nu(COO^-)_s]$ is about 132 cm^{-1}, suggesting the presence of the chelated type of 1,3-pdta ligand. This is consistent with the structural analysis which shows more chelate bonds in the 1,3-pdta ligands. These changes confirm that the oxygen atoms from the carboxy groups of 1,3-pdta are coordinated with the centre ions. The ν(C–N) of complexes **1–5** near 1100 cm^{-1} displays an obvious blue-shift compared with that of H_4pdta, suggesting that the nitrogens of pdta are coordinated to the centre ions.

Thermogravimetric analyses (TGA)

The thermal stability and decomposition patterns of the complexes were investigated by thermogravimetric analyses. The TG-DTG curves of complexes **1** and **5** are listed in Fig. S12† and Fig. 6. The first part of the large weight loss starts at 80 and 94 °C, which corresponds to the loss of crystallized water molecules for **1** and **5**, respectively. The coordinated water molecules decompose at 120, 144 and 192 °C for **1** and **5**. Then the weight remains steady. The largest weight loss starts from 299 and 366 °C for **1** and **5**, respectively, where the ligand is decomposed step by step in this process. At 690 and 731 °C, there is a small weight loss, which may correspond to the conversion of lanthanum oxocarbonate to lanthanum oxide for **1** and **5**, respectively (Fig. 6 and S12†), the latter shows a strong interaction with strontium. At last, there exists a small weight loss at around 850 °C, which is assigned to the thermal decomposition of the strontium carbonate of $[La_2(1,3\text{-pdta})_2(H_2O)_4]_n[Sr_2(H_2O)_6]_n[La_2(1,3\text{-pdta})_2(H_2O)_2]_n{\cdot}18nH_2O$ (**5**).

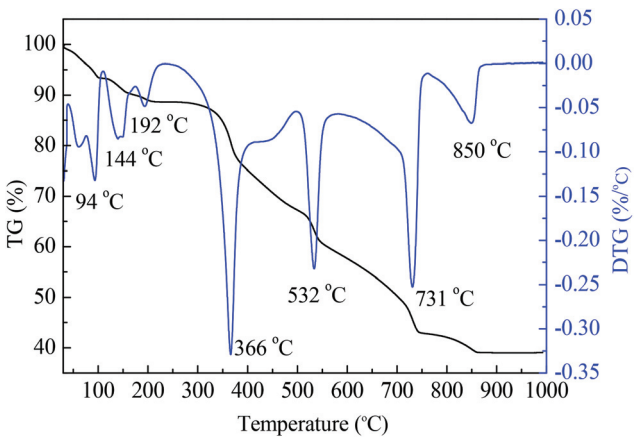

Fig. 6 TG-DTG curves of $[La_2(1,3\text{-pdta})_2(H_2O)_4]_n{\cdot}[Sr_2(H_2O)_6]_n{\cdot}[La_2(1,3\text{-pdta})_2(H_2O)_2]_n{\cdot}18nH_2O$ (**5**).

Characterization of lanthanum and strontium lanthanum catalysts

Complexes **1** and **5** were calcined under atmospheric air at 600 °C for 6 h to obtain the final catalysts. The X-ray diffraction patterns of the samples before and after reaction are shown in Fig. 7. Before reaction, the diffraction peaks were assigned to lanthanum oxocarbonate $La_2O_2CO_3$ (PDF# 84-1963) for **1**. While the diffraction peaks were assigned to a mixture of La_2O_3 (PDF# 74-2430), $SrCO_3$ (PDF# 84-1778) and $La_2O_2CO_3$ (PDF# 84-1963) for **5**. The two thermal decomposition products contain carbonates. This is because of the alkaline nature of the centre ions, and the coordinated carboxy groups increase the alkalescence, which is consistent with the results of the thermogravimetric analyses. In addition, the intensity of the product from **5** decreased obviously and the width became broadened compared with that of **1**, which indicated that the particle sizes of **5** decreased. After the reaction, there are no obvious changes in **1**, this indicated that the lanthanum oxocarbonate from **1** is relatively stable. While the intensities of La_2O_3 (PDF# 74-2430) increased and the widths of the peaks narrowed for **5**, this showed that the particle sizes from **5**

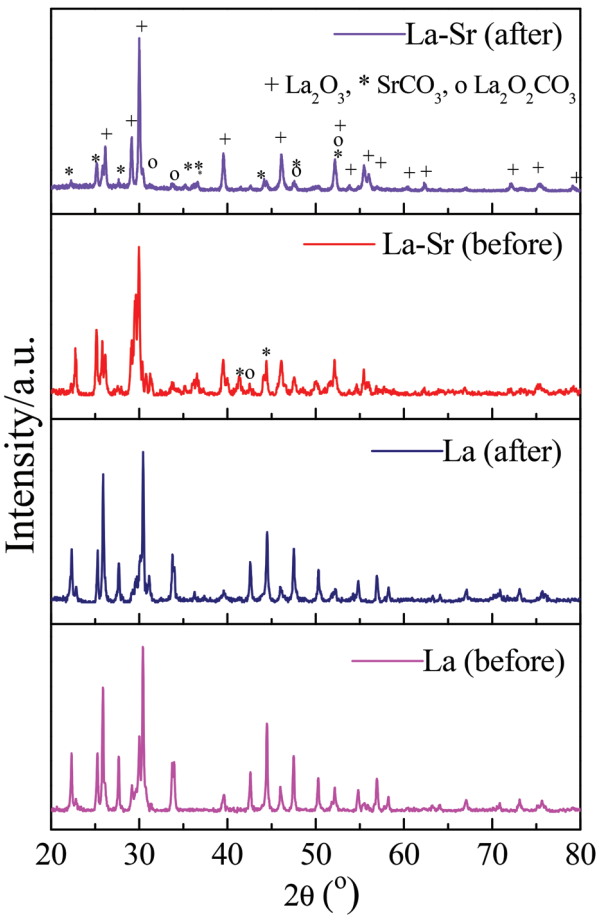

Fig. 7 The X-ray diffraction patterns of the thermal decomposition products from $(NH_4)_2[La_2(1,3\text{-pdta})_2(H_2O)_4]{\cdot}8H_2O$ (**1**) and $[La_2(1,3\text{-pdta})_2(H_2O)_4]_n{\cdot}[Sr_2(H_2O)_6]_n{\cdot}[La_2(1,3\text{-pdta})_2(H_2O)_2]_n{\cdot}18nH_2O$ (**5**) (before and after catalytic reactions).

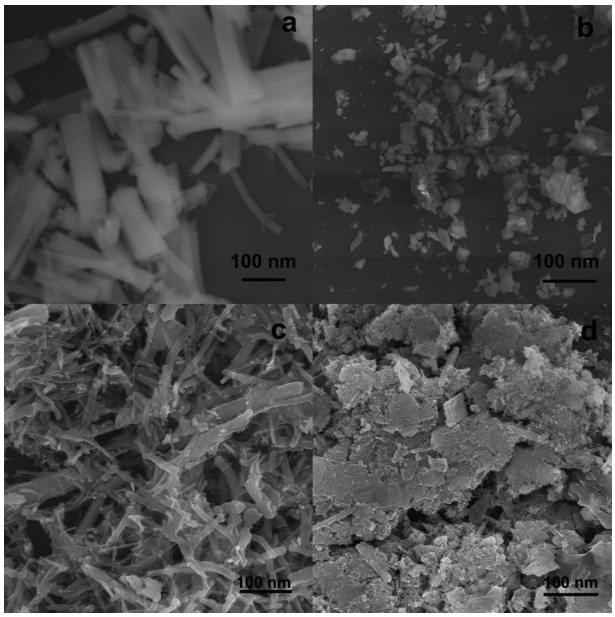

Fig. 8 The SEM images of the calcined products from **1** and **5**. (a) The thermal decomposition product from **1**; (b) the thermal decomposition product from **5**; (c) the thermal decomposition product of **1** after catalytic reaction; (d) the thermal decomposition product of **5** after catalytic reaction.

increased obviously after reaction. Moreover, the intensity of lanthanum oxocarbonate $La_2O_2CO_3$ weakened, which means the amount of $La_2O_2CO_3$ decreased.

The SEM images of the products from **1** and **5** are shown in Fig. 8 before and after the reactions. As shown in the images, the morphology of the lanthanum oxocarbonate from **1** is a rod-like shape after decomposition, while that from **5** is grainy, and particle sizes from **5** are smaller than that from **1**, which is consistent with the XRD results. After the reaction, the morphology of lanthanum oxocarbonate from **1** also possesses a rod-like shape, but not so uniform. While there are a lot of agglomerations for **5**, and the particle sizes grow quite obviously.

Catalytic activities for the oxidative coupling of methane (OCM)

As shown in Fig. 9, the catalytic performances of the thermal decomposition products from **1** and **5** towards the OCM reactions were investigated at temperatures ranging from 550 to 800 °C. The detailed catalytic activity data are shown in Table S1.† At 550 °C, there is no conversion of methane for lanthanum oxocarbonate from **1**, while the conversion of methane and the selectivity to C_2 are 12.6% and 24.1% respectively for **5**. The catalytic performances increased rapidly with the increase of the temperature. At 700 °C, the conversion of methane and the selectivity to C_2 reach 23.0% and 45.8% for the lanthanum oxocarbonate from **1**, which are much better than that of conventional bulk La_2O_3.[16] For **5**, the conversion of methane and selectivity to C_2 are 29.7% and 51.7% respectively at 750 °C, which are also better than that of the

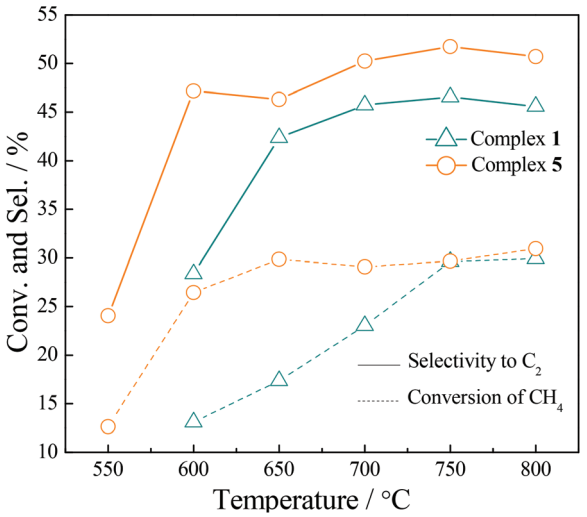

Fig. 9 Catalytic activity of the thermal decomposition products from **1** and **5** towards the oxidative coupling of methane (CH_4/O_2 = 2.8/1, GHSV = 15 000 $mL \cdot g^{-1} \cdot h^{-1}$).

bulk La–Sr sample.[17] In addition, the catalytic performances of the thermal products from **5** are much better than that of lanthanum oxocarbonate from **1**. This may be attributed to the decreased particle sizes, which can be observed in the SEM images (Fig. 2), and the increased number of alkaline sites with the addition of strontium. This is consistent with the previously reported results that alkaline earth oxides, especially strontium, have excellent promoting effects on the catalytic activity of La_2O_3 towards to the OCM reaction,[18] while the OCM catalytic performance of the lanthanum oxocarbonate from **1** is also interesting.

Conclusions

In summary, four dimeric 1,3-propanediaminetetraacetato lanthanide complexes $(NH_4)_2[Ln_2(1,3\text{-pdta})_2(H_2O)_4]\cdot 8H_2O$ [Ln = La, **1**; Ce, **2**] and $K_2[Ln_2(1,3\text{-pdta})_2(H_2O)_4]\cdot 11H_2O$ [Ln = La, **3**; Ce, **4**] and a novel two-dimensional strontium 1,3-propanediaminetetraacetato lanthanum complex (**5**) were isolated and characterized. The thermal decomposition products from **1** and **5** show good catalytic activities for the oxidative coupling of methane. Strontium had an excellent promoting effect, and lanthanum oxocarbonate also shows an interesting result on the catalytic reaction.

Acknowledgements

This work was financially supported by the National Science Foundation of China (21133007, 21033006, 21373169), the Ministry of Science and Technology of China (2010CB732303, 2012CB214900) and PCSIRT (no. IRT1036).

Notes and references

1 (*a*) J. Yang, Q. Yuo, G. D. Li, J. J. Cao, G. H. Li and J. S. Chen, *Inorg. Chem.*, 2006, **45**, 2857–2865; (*b*) X.-L. Li, C.-L. Chen, H.-P. Xiao, A.-L. Wang, C.-M. Liu, X. Zheng, L.-J. Gao, X.-G. Yang and S.-M. Fang, *Dalton Trans.*, 2013, **42**, 15317–15325; (*c*) J. Tian, B. Li, X. Zhang, X. Li, X. Li and J. Zhang, *Dalton Trans.*, 2013, **42**, 8504–8511; (*d*) C. Benelli and D. Gatteschi, *Chem. Rev.*, 2002, **102**, 2369–2387.

2 (*a*) I. Hemmila and V. Laitala, *J. Fluoresc.*, 2005, **15**, 529–542; (*b*) M. Elhabiri, R. Scopelliti, J. C. G. Bunzli and C. Piguet, *J. Am. Chem. Soc.*, 1999, **121**, 10747–10762; (*c*) C. Piguet, J. C. G. Bunzli, G. Bernardinelli, G. Hopfgartner, S. Petoud and O. Schaad, *J. Am. Chem. Soc.*, 1996, **118**, 6681–6697.

3 (*a*) S. Shirvani-Arani, S. J. Ahmadi, A. Bahrami-Samani and M. Ghannadi-Maragheh, *Anal. Chim. Acta*, 2008, **623**, 82–88; (*b*) Y. Zhao, L.-L. Liang, K. Chen, T. Zhang, X. Xiao, Y.-Q. Zhang, Z. Tao, S.-F. Xue and Q.-J. Zhu, *CrystEngComm*, 2013, **15**, 7987–7998; (*c*) C. Y. Li, J. Z. Gao, W. Yang, B. Y. Li and H. T. Liu, *Rare Met.*, 2000, **19**, 136–140; (*d*) H. L. Nekimken, B. F. Smith, G. D. Jarvinen and C. S. Bartholdi, *Solvent Extr. Ion Exch.*, 1992, **10**, 419–429.

4 (*a*) J. C. G. Bunzli, *Acc. Chem. Res.*, 2006, **39**, 53–61; (*b*) M. Bottrill, L. K. Nicholas and N. J. Long, *Chem. Soc. Rev.*, 2006, **35**, 557–571; (*c*) J. A. Peters, J. Huskens and D. J. Raber, *Prog. Nucl. Magn. Reson. Spectrosc.*, 1996, **28**, 283–350; (*d*) D. H. Powell, O. M. NiDhubhghaill, D. Pubanz, L. Helm, Y. S. Lebedev, W. Schlaepfer and A. E. Merbach, *J. Am. Chem. Soc.*, 1996, **118**, 9333–9346.

5 (*a*) A. L. Kustov, O. P. Tkachenko, L. M. Kustov and B. V. Romanovsky, *Environ. Int.*, 2011, **37**, 1053–1056; (*b*) A. Rath, E. Aceves, J. Mitome, J. Liu, U. S. Ozkan and S. G. Shore, *J. Mol. Catal. A: Chem.*, 2001, **165**, 103–111; (*c*) T. Mirkovic, M. A. Hines, P. S. Nair and G. D. Scholes, *Chem. Mater.*, 2005, **17**, 3451–3456; (*d*) T. J. Boyle, R. Raymond, D. M. Boye, L. A. M. Ottley and P. Lu, *Dalton Trans.*, 2010, **39**, 8050–8063; (*e*) D. Liu and D. Cui, *Dalton Trans.*, 2011, **40**, 7755–7761; (*f*) S. Mishra, G. Ledoux, E. Jeanneau, S. Daniele and M.-F. Joubert, *Dalton Trans.*, 2012, **41**, 1490–1502; (*g*) A. J. Wooles, D. P. Mills, W. Lewis, A. J. Blake and S. T. Liddle, *Dalton Trans.*, 2010, **39**, 500–510.

6 (*a*) K. Kili, L. Hilaire and F. Le Normand, *Phys. Chem. Chem. Phys.*, 1999, **1**, 1623–1631; (*b*) N. B. Wong, K. C. Tin, Q. N. Zhu, M. Z. Zhang and X. Q. Qiu, *J. Chem. Technol. Biotechnol.*, 1996, **67**, 164–168; (*c*) Y. Guo, G. Lu, Z. Zhang, S. Zhang, Y. Qi and Y. Liu, *Catal. Today*, 2007, **126**, 296–302.

7 (*a*) A. G. Dedov, G. D. Nipan, A. S. Loktev, A. A. Tyunyaev, V. A. Ketsko, K. V. Parkhomenko and I. I. Moiseev, *Appl. Catal., A*, 2011, **406**, 1–12; (*b*) L. Qiu, T. Ichikawa, A. Hirano, N. Imanishi and Y. Takeda, *Solid State Ionics*, 2003, **158**, 55–65; (*c*) W. Wang, C. Su, R. Ran and Z. Shao, *J. Power Sources*, 2011, **196**, 3855–3862; (*d*) A. Goel, A. A. Reddy, M. J. Pascual, L. Gremillard, A. Malchere and J. M. F. Ferreira, *J. Mater. Chem.*, 2012, **22**, 10042–10054.

8 (*a*) B. J. Clapsaddle, B. Neumann, A. Wittstock, D. W. Sprehn, A. E. Gash, J. H. Satcher Jr., R. L. Simpson and M. Baeumer, *J. Sol-Gel Sci. Technol.*, 2012, **64**, 381–389; (*b*) J. P. Boilot, T. Gacoin and S. Perruchas, *C. R. Chim.*, 2010, **13**, 186–198; (*c*) Q. Kuang, Z.-W. Lin, W. Lian, Z.-Y. Jiang, Z.-X. Xie, R.-B. Huang and L.-S. Zheng, *J. Solid State Chem.*, 2007, **180**, 1236–1242; (*d*) L. Armelao, G. Bottaro, G. Bruno, M. Losurdo, M. Pascolini, E. Soini and E. Tondello, *J. Phys. Chem. C*, 2008, **112**, 14508–14512.

9 M. L. Panchula and M. Akinc, *J. Eur. Ceram. Soc.*, 1996, **16**, 833–841.

10 (*a*) P. Ji, M. Xing, S. Bagwasi, B. Tian, F. Chen and J. Zhang, *Mater. Res. Bull.*, 2011, **46**, 1902–1907; (*b*) G. Jia, C. Zhang, L. Wang, S. Ding and H. You, *J. Alloys Compd.*, 2011, **509**, 6418–6422; (*c*) F. Chen, Y.-J. Zhu, K.-W. Wang and Y.-B. Pan, *Curr. Nanosci.*, 2009, **5**, 266–272.

11 (*a*) S. Sohn, Y. Kwon, Y. Kim and D. Kim, *Powder Technol.*, 2004, **142**, 136–153; (*b*) Happy, A. I. Y. Tok, L. T. Su, F. Y. C. Boey and S. H. Ng, *J. Nanosci. Nanotechnol.*, 2007, **7**, 907–915; (*c*) J. G. Li, T. Ikegami, T. Mori and Y. Yajima, *J. Mater. Res.*, 2003, **18**, 1149–1156.

12 (*a*) G. O. Siqueira, A. d. O. Porto, M. M. Viana, H. V. da Silva, Y. G. de Souza, H. W. Alves da Silva, G. M. de Lima and T. Matencio, *Phys. Chem. Chem. Phys.*, 2013, **15**, 16236–16241; (*b*) I. Melian-Cabrera, M. L. Granados and J. L. G. Fierro, *Phys. Chem. Chem. Phys.*, 2002, **4**, 3122–3127; (*c*) G. A. A. Costa, M. C. Silva, A. C. B. Silva, G. M. de Lima, R. M. Lago and M. T. C. Sansiviero, *Phys. Chem. Chem. Phys.*, 2000, **2**, 5708–5711; (*d*) M. F. Pinheiro da Silva, F. M. de Souza Carvalho, T. d. S. Martins, M. C. de Abreu Fantini and P. C. Isolani, *J. Therm. Anal. Calorim.*, 2010, **99**, 385–390; (*e*) L. Si, L. Yue and D. Jin, *Cryst. Res. Technol.*, 2011, **46**, 1149–1154.

13 M.-L. Chen, Y.-C. Guo, F. Yang, J.-X. Liang, Z.-X. Cao and Z.-H. Zhou, *Dalton Trans.*, 2014, **43**, 6026–6031.

14 (*a*) G. M. Sheldrick, *SHELXS-97, SHELXL-97, and SHELXTL/PC, Programs for solution and refinement of crystal structures*, University of Göttingen, Göttingen, 1997; (*b*) A. J. C. Wilson, *International Tables for Crystallography*, 1995.

15 K. Nakamoto, *Infrared and Raman Spectra of Inorganic and Coordination Compounds: Part B. Applications in Coordination, Organometallic, and Bioinorganic Chemistry*, John Wiley & Sons, Inc., New Jersey, 2009.

16 H. L. Wan, X. P. Zhou, W. Z. Weng, R. Q. Long, Z. S. Chao, W. D. Zhang, M. S. Chen, J. Z. Luo and S. Q. Zhou, *Catal. Today*, 1999, **51**, 161–175.

17 R. Q. Long, *Doctoral Dissertation*, Xiamen University, -1997.

18 V. R. Choudhary, S. A. R. Mulla and V. H. Rane, *J. Chem. Technol. Biotechnol.*, 1998, **72**, 125–130.